

## **Chapter 3. Radar Search and Overview of Detection in Interference**

**James A Scheer**

### **3.1 Introduction**

Though there are many specific applications for radar systems, there are three general functions that radars perform, with all the specific applications falling into one or more of these general functions. The three primary functions are *search*, *track*, and *image*. The radar search mode implies the process of target detection. Target tracking implies that the radar makes measurements of the target state in range, azimuth angle, elevation angle, and Doppler frequency offset. The tracking software then develops an accurate state vector (position and velocity) for the target, typically in a Cartesian coordinate system of North, East, and down. That state estimate then becomes an integral part of a fire control system, directing a weapon, or cueing another sensor to the target state. Once a target is detected and in track, depending on the application for the radar, an imaging mode may be implemented, developing high resolution data in range, azimuth, elevation, and sometimes Doppler.<sup>1</sup> This would support target classification, discrimination, and or identification functions. The present chapter is designed to provide the detailed description of the radar processes associated with supporting the search and detect functions. Sensor measurements are covered in Chapter 18, the track function is described in Chapter 19 and the two-dimensional imaging function is described in Chapters 20 and 21.

Some systems are designed to perform two or three of these tasks. One way to do this is with multiple radar systems, one optimized for search and another for track. In many cases, however, allowable space and prime power limitations do not allow for multiple radar systems. If a single radar system has to perform both the search function and the track function, then there is likely a compromise required in the design. In the following sections it will be seen that some of the features of a good search radar will not be

---

<sup>1</sup> Radars whose primary function is imaging generally do not have search and track modes. Some new systems combine imaging with detection and tracking of targets within the image.

desirable in a good track radar. These same features do not necessarily necessitate a compromise in the imaging mode, however.

In this chapter the reader will learn how a radar performs a volume search, given a limited instantaneous field of view determined by the antenna beamwidth; the fundamental analysis required to relate signal-to-noise ratio (SNR) to  $P_D$  and  $P_{FA}$ ; and the reasons for using more than one dwell time at each beam position, which include the need to mitigate blind ranges and blind Doppler shifts and to resolve ambiguous range and velocity measurements. It will be determined whether it is more efficient to dwell for multiple dwell periods or use extended dwell times within a coherent processing interval (CPI) for equivalent detection performance.

### **3.2 Search Mode Fundamentals**

A search radar is designed to look for targets, when and where there is no *a priori* knowledge of the target existence. It is designed to search for a given target type in a given solid angle volume, out to a given slant range, in a specified amount of time. These parameters are derived from the system application requirements, so there is no way to develop a set of requirements here. However, the situation is much like a prison search light which is illuminating a prison yard, looking for prisoners trying to escape over the fence. The light must scan by the area in a time short enough that a prisoner can't run from the building to the fence and escape between search light scans. The following several sections will develop the methodology to determine radar requirements for a given search requirement.

It is important to realize that use of an electronically scanned antenna (ESA) beam (phased array) and a mechanically scanned antenna beam lead to somewhat different search patterns. The mechanically scanned beam must scan in one dimension at a time, turning around to scan in the other direction at the end of the scan volume. The scanning motion is continuous, smoothly transitioning from one beam position to the next, as the radar system performs the detection process. An electronically scanned beam can step

incrementally from one position to the next, and these sequential positions do not need to be contiguous in space.

### 3.2.1 Search Volume

A search radar is designed to search a solid angle volume at a given rate. The volume may be as small as a few degree elevation sector over a 90° azimuth sector. An example of a small search volume is the AN/TPQ-36 and -37 Firefinder radars. They are designed to search just above the horizon over a 90° azimuth sector, looking for artillery rounds out to about 30 km range. If artillery rounds are detected, then the radar tracks them long enough to estimate the point of launch so that counterfire can be issued. The Firefinder is a phased array radar, so that the search and track functions are interleaved. The search function is not interrupted for long periods of time. Another example of a limited search volume is a ship self defense system, in which the radar is looking for incoming cruise missiles over all azimuth angles, but only at elevations at or near the sea surface. The search volume for these relatively narrow elevation sectors is often referred to as a search “fence”, in reference to the general shape of the search pattern.

Some search radars are designed to search a much larger volume, up to a full hemisphere ( $4\pi$  steradians of solid angle). This might be the case for radars searching for incoming ballistic missiles or high-flying anti-ship missiles. In this case, it is expected that the time allowed to complete a single complete search pattern would be longer than that for a Firefinder-like application.

### 3.2.2 Total Search Time

For an ESA, the total frame search time  $T_{fs}$  for a given volume is determined by the number of beam pointing positions  $m$  required to see the entire search volume contiguously, and the dwell time  $T_d$  required at each beam position to achieve the probability of detection  $P_d$  and probability of false alarm  $P_{FA}$  required:

$$T_{fs} = mT_d \quad (3.1)$$

The number of beam positions depends on the total solid angle to be scanned ( $\Omega$ ) and the product of the azimuth and elevation beamwidths  $\theta_{az}$  and  $\theta_{el}$ :

$$m = \frac{\Omega}{\theta_{az}\theta_{el}} \quad (3.2)$$

For example, if the search volume is a sector covering  $90^\circ$  in azimuth and  $4^\circ$  in elevation, and the azimuth and elevation beamwidths are both  $2^\circ$ , then there will be 45 beam positions in azimuth and 2 beam positions in elevation, resulting in 90 total beam positions. Figure 3-1 depicts a sequence of discrete beam positions designed to cover a specific scan volume having two rows. (note: not every beam position is depicted, for clarity.)

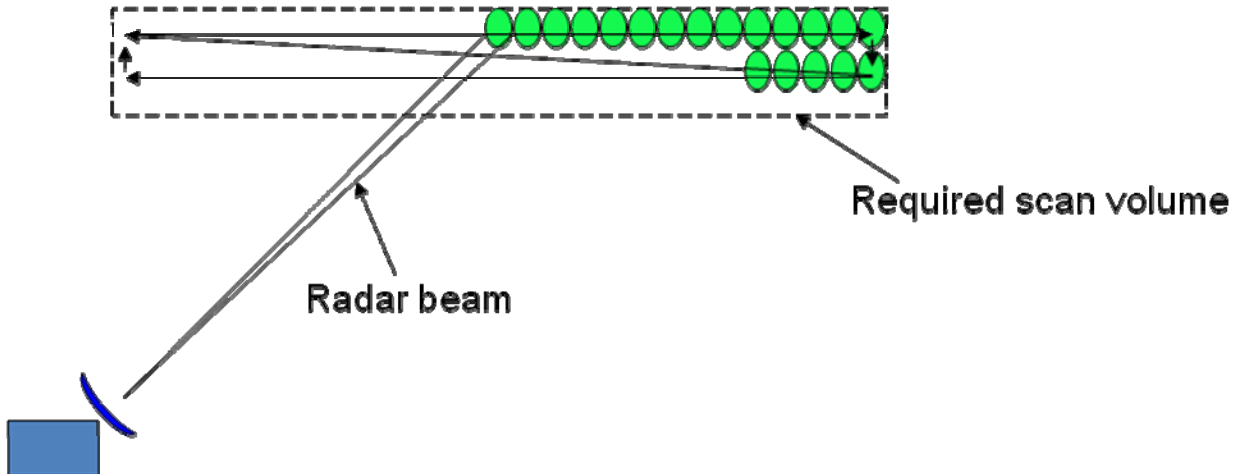


Figure 3-1. Radar antenna beam scanning in the search mode.

Combining Eqs. (3.1) and (3.2), the total frame scan time is

$$T_{fs} = \frac{\Omega T_d}{\theta_{az}\theta_{el}} \quad (3.3)$$

If, say, 3 dwells are required (for reason that will be discussed later) at 2 msec per dwell at each beam position, then the total scan time for 90 beam positions is 540 msec. This figure ignores the time it takes for the beam to move from one position to the next, which, for a modern electronically scanned antenna, is short relative to the total dwell time.

In this example, there would be antenna beams spaced at the -3dB point on the beam (-6 dB round trip) which would produce a *beamshape loss*, or *scalping loss*,<sup>2</sup> because the target would not necessarily be at the peak of the beam at detection. One way to reduce this loss is to reduce the beam spacing, increasing the number of beam positions.

For a mechanically scanned antenna, the scan time is determined by the angular scanning rate of the beam, and the total angle required. The dwell time can be no longer that the time the beam is pointed at a given position, and must be consistent with the detection performance, in the same way as for the ESA. There may be several dwells, or coherent processing intervals (CPIs) during the time the beam is pointed at a potential target position.

### 3.2.3 Phased Array Antenna Issues

When using an electronically scanned antenna for performing the search operation, the beamwidth and gain change with scan angle.<sup>3</sup> This change in beamwidth and gain must be considered in designing the search program. As the beam is scanned away from normal to the plane of the aperture the gain reduces because of two effects. The first is that the effective aperture (the projection of the antenna surface area in the direction of the beam scan) is reduced by the cosine of the scan angle. For a modest scan of, say, 10 degrees, this effect is mild. However, for a 45 degree scan angle the cosine is 0.707, resulting in a gain reduction of about 1.5 dB. For a fixed dwell time, this results in an SNR reduction of 3 dB, because the gain is squared in the radar range equation.

---

<sup>2</sup> This effect is often called *straddle loss* in range and Doppler processing.

<sup>3</sup> See Chapter 9 for a more detailed discussion of these effects.

The second effect which reduces the gain is related to the fact that each of the radiating elements in the antenna has its own beam pattern, which is at its peak broadside to the aperture but falls off with scan angle. For small scan angles this again represents a marginal reduction in gain. However, for large scan angles it can be significant. This loss adds to the effective aperture loss.

The consequence of this scan loss is that the detection performance will degrade as the scan angle decreases. If the radar's detection performance is required to be equally good at all scan angles, then designing the system to achieve this performance at the highest scan angle, where the losses are greatest, will result in it performing well beyond the requirements at a low scan angle. One way to normalize performance at all scan angles is to lengthen the coherent processing interval (dwell time) at wide angles and shorten it at low scan angles in order to counteract the gain variations. This is usually done in quantum steps. For example, a system might have a dwell time of  $T_d$  at scan angles of zero to 15 degrees,  $2T_d$  at 15 to 30 degrees,  $4T_d$  at 30 to 45 degrees, and so forth.

In the search mode, one usually has to account for the beamshape loss, since the target may be at any arbitrary position in the beam when detection is attempted. In addition to the gain loss, there is a widening of the beamwidth as the electronically scanned beam is scanned away from normal due to the reduced effective aperture. This widening partially offsets the effect of gain loss, because the beamshape loss is reduced. The designer can either take advantage of this reduced loss to reduce the required dwell time at off-normal beam positions, or reduce the total scan time required by increasing the antenna beam step size to maintain a constant beamshape loss.

#### 3.2.4 Search Regimens

Some radar systems have to perform multiple functions nearly simultaneously. This is done by interleaving these functions at a high rate. A prime example is the case in which a radar has to continue to search a volume while also tracking targets that have previously been detected, or that represent a threat. Though multifunction radars are becoming more

popular, the design for such a system represents a compromise compared to a system that has to perform only a search function or only a track function.

For example, longer wavelengths are favored for search radars and shorter wavelengths are favored for track functions, as discussed in Ch. 2. As noted earlier, available space and prime power often do not allow for more than one radar for all the required functions. A fixed ground-based air defense system might have the resources to employ multiple radars, but a mobile artillery finding radar may not. The latter system must be small, mobile, and must run on a single 60 kVA generator. As another example, a surface ship-based system might have several radars onboard, but a forward-looking airborne interceptor system has space for only one aperture.

With the technology improvements associated with electronically scanned antennas (phased arrays), it is now practical to incorporate multiple functions in a single radar system. The most candidates to combine are the search and track functions. There are two distinctly different approaches to combining the search and track functions in a single system. One approach is called *search and track*, and the other is *track-while-scan*.

#### 3.2.4.1 *Track-While-Scan*

In the track-while-scan (TWS) mode, the antenna search protocol is established and never modified. When a target is detected as the beam scans in the search volume, a track file is established. The next time the antenna beam passes over this target, a new measurement is made and its track file is updated. Since the beam scan sequence is not changed to accommodate detected targets, this technique does not require the scanning agility of an electronically scanned antenna. As the beam continues to search the volume and more targets are detected, new track files are established for these targets and updated when the beam scans by them again. In this mode, an arbitrarily large number of targets can be tracked (1000 or more), limited only by the computer memory and track filter throughput required. The TWS approach is used for air marshalling<sup>4</sup>, air traffic

---

<sup>4</sup> The US Navy has a requirement to monitor and control aircraft in the vicinity of an aircraft carrier. This procedure is termed “marshalling”.

control, and airport surveillance applications, among others. Many of these systems use mechanically scanned antennas.

As an example, an air surveillance radar antenna typically has a wide elevation beamwidth to provide coverage at all altitudes, but a narrow azimuth beamwidth. The antenna may rotate at 10 revolutions per minute (RPM) as it searches a 360 degree azimuth sector. This means that the beam will be pointed at any given azimuth direction once every 6 seconds, and the track file for a given target will be updated with new sensor measurements every 6 seconds. This rate is adequate for benign non-threatening targets such as commercial aircraft, but not for immediately threatening targets such as incoming missiles, *etc.* An adaptive, more responsive search and track technique for this situation is the *search and track* mode.

#### 3.2.4.2 *Search and Track*

*Search and track* systems require that the antenna beam be electronically scanned, because the beam must be capable of being moved rapidly between arbitrary positions to optimize the tracking mode. In this mode, the radar sequencer (a computer control function often called the *resource manager*) first establishes a search pattern designed to optimize the search function according to the search parameters (search volume, search frame time, prioritized sectors, *etc.*) If a target is detected in the search volume, then some of the radar resources are devoted to tracking this target. For instance, some percentage of the dwells each second might be assigned to target track updates. As a simple example, consider a radar searching a volume defined as a 90 degree azimuth sector and a 4 degree elevation sector. When a target is detected, the resource manager allocates whatever resources are required, based on target size, distance, speed, *etc.*, for a high quality track. Assume the resource manager devotes 5% of the dwells to providing measurements to the track algorithm for that target. Thus 95% of the radar resources are left to continue the search, slowing the search somewhat. If another target is subsequently detected, another 5% of the resources may be devoted to tracking this second target, leaving 90% of the original radar dwells for searching and further slowing the search. If ten targets are being tracked, each using 5% of the radar resources, only



50% of the resources are left to continue the search. In this case, the search frame time will double compared to the original frame time.

This example makes clear that in search and track, there is a limit to the number of targets that can be tracked simultaneously before there remains too few of the radar resources to continue an effective search. If the search frame time becomes too long, then targets of interest may get through the angular positions being searched between scans. It is the responsibility of the resource manager to strike an appropriate balance between the search frame time and the number of target tracks maintained.

Some systems combine both search and track and track-while-scan functions. The rationale for this is as follows. The frequent updates and agility of a search and track system are required to accurately track targets that represent short-term threats and may have high dynamics (velocities and accelerations). Examples of such targets include incoming threats such as anti-ship missiles, fast, low RCS, low altitude cruise missiles, and enemy artillery such as mortars and rockets. Radar systems designed to detect and track such targets are very sensitive, that is they are able to detect low RCS targets at long range in the presence of high RCS clutter. They also typically perform target identification functions by analyzing the target amplitude and Doppler characteristics. Such a system is likely to be a medium PRF pulse Doppler radar.

If a target is detected and *confirmed* or *qualified* to be a true target (as opposed to a false alarm), then the target identification process is initiated. If the target is determined to be a threat rather than benign, a track file is initiated. This track initiation process consumes time for each target detected. Due to the sensitivity of these radar systems, target detections can occur not only for potential threat targets such as ground moving vehicles and helicopters, but also for birds, insects, and even turbulent air. Insects and turbulent air will only be detected at short range, however, for a range ambiguous medium PRF system, a small target that is apparently at close range may be a true threat target at a longer range.

There may be many such detections in a single search scan, consuming a large fraction of the radar timeline in the target qualification process. For example, if it takes 100 msec to qualify a target and there are 100 potential target detections in a scan, then the radar will consume the next 10 seconds qualifying targets. Once the “uninteresting” targets are identified, they must still be continually tracked, or else they will be detected again on subsequent scans and have to be requalified repeatedly. However, a high precision track is not required for these targets. Consequently, a track-while-scan mode can be used to maintain tracks on these targets without consuming large amounts of radar timeline.

### **3.3 Overview of Detection Fundamentals**

#### ***3.3.1 Overview of the Threshold Detection Concept***

The concept of “detection” of a target involves deciding, for each azimuth/elevation beam position, and for each Doppler “bin” in every range bin, whether a target of interest exists in that position and bin. The technique may be as simple as an operator looking at a display deciding if a given cell is “bright” enough, relative to the surrounding interference (noise or clutter) to be a target of interest. In most modern radar systems, detection is performed automatically, in the signal/data processor. It is accomplished by establishing a threshold signal level (voltage) on the basis of the current interference level, and then deciding on the presence of a target by comparing the signal level in every cell to that threshold. If the signal level exceeds the threshold, then the presence of a target is declared. If the signal does not exceed the threshold, then no target is declared. This concept is shown in Fig. 3-2.

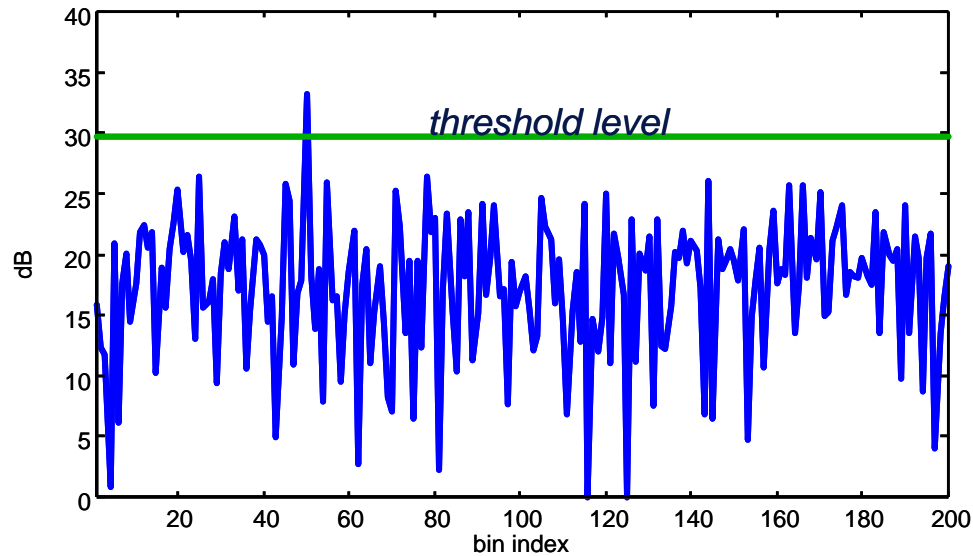


Figure 3-2. Concept of threshold detection. In this example, a target would be declared at bin #50.

If the interference is known to consist only of thermal noise in the receiver, then the gains can be set such that the noise voltage will be at a known level. The detection threshold can then be set at a fixed voltage, far enough above that noise level to keep the probability of a false alarm (threshold crossing due to noise instead of a target) at an acceptably level. However, the interference is seldom this well known.

In many radars the interference consists not only of receiver noise, but also of clutter and jamming signals. Consequently, the interference level can vary by many dB during operation, so that a fixed threshold level is not feasible. Particularly in modern radars, the threshold is often adaptive, automatically adjusting to the local interference level so as to result in a constant false alarm rate (CFAR). The target signal, when present, must exceeds the threshold In order to be detected.

The description so far is of detection on the basis of amplitude alone, so that the amplitude of the target signal must exceed that of the interfering signal by a sufficient amount. When the dominant interference source is clutter and its amplitude exceeds that of the target signal, spectral signal processing is employed (moving target indication

and/or pulse Doppler processing) to reduce the interference level below that of the target signal. In cases where the dominant interference is jamming and its level exceeds that of the target, angle-of-arrival processing (adaptive beamforming) is used. Systems suffering significant clutter and jamming interference may use a combination of both called space-time adaptive processing (STAP). The detection process is performed on the output of such processors. Each of these more advanced techniques is described in subsequent chapters.

The radar user is usually most interested in knowing (or specifying) the probability of detecting a given target ( $P_D$ ) and the probability of a false alarm ( $P_{FA}$ ) caused by interference. This chapter introduces the process for developing the relationship between  $P_D$ ,  $P_{FA}$  and SNR. Curves describing these relationships are often called *receiver operating curves* or *receiver operating characteristics* (ROCs).

The intent of the remainder of this chapter is to build an understanding of the issues associated with detecting a desired target in the presence of unavoidable interfering signals. The primary emphasis will be on the simplest case of a non-fluctuating target signal, and noise-like (*i.e.* Rayleigh-distributed) interference, though some extensions will be mentioned. Chapter 14 extends the topic of detection to include the effects of the Swerling fluctuating target models, and Chapter 16 describes the implementation and performance of systems that use CFAR techniques to set the threshold level adaptively.

### 3.3.2 Probabilities of False Alarm and Detection

The interference (at least noise, possibly also clutter and jamming) at the receiver output is a randomly varying voltage. Realistic targets also present echo voltages that vary randomly from pulse to pulse. However, even if the target is modeled as a constant echo voltage, the output voltage of the receiver when a target is present is the combination of the target echo and noise, and so still varies randomly. Therefore the process of detecting the presence of a target on the basis of the signal voltage is a statistical process, with a

probability of success usually less than unity, and some probability of false alarm usually greater than zero.

The fluctuating interference and target-plus-interference voltages  $v$  are characterized in terms of their probability density functions (PDFs)  $p(v)$ , which are functions describing the relative likelihood that a random variable will take on various values. For example, the Gaussian or normal PDF of Fig. 3-3 shows that the voltage  $v$  can take on positive and negative values with equal likelihood, can range from large negative to large positive values, but is more likely to take on values near zero than larger values. The likelihood of taking on values outside of the range of about -2 to +2 is quite small in this example.

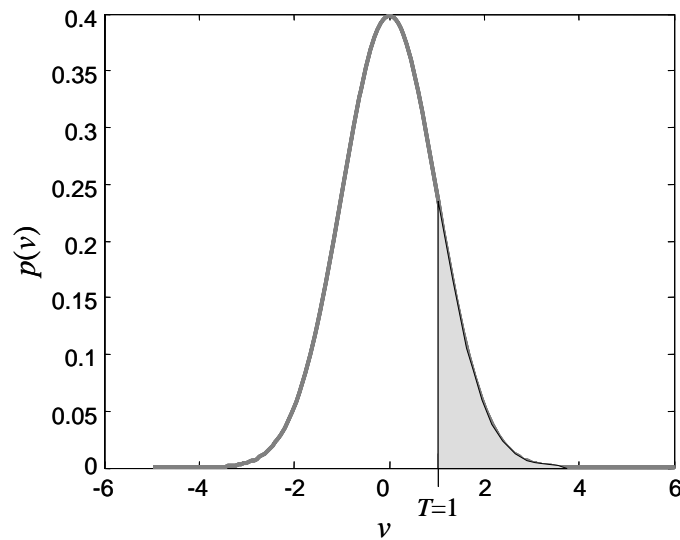


Figure 3-3. Gaussian PDF for a voltage  $v$ .

Probability density functions are used to compute probabilities. For example, the probability that the random variable  $v$  exceeds some threshold voltage  $T$  is the area under the PDF for in the region where  $v > T$ , which is

$$\text{Probability}\{v > V_t\} = \int_{V_t}^{\infty} p(v) dv \quad (3.4)$$

To apply this, suppose the PDF of the interfering signal is denoted as  $p_i(v)$  and a voltage threshold  $V_t$  is established at some level, usually several standard deviations above the interference mean, to prevent false alarms. The false alarm probability  $P_{FA}$  is the integral of the interference probability density function from the threshold voltage to positive infinity.

$$P_{FA} = \int_{V_t}^{\infty} p_i(v) dv \quad (3.5)$$

By increasing or decreasing the threshold level  $V_t$ ,  $P_{FA}$  can be decreased or increased. Thus,  $P_{FA}$  can be set at any desired level by proper choice of  $V_t$ .

Once the threshold is established on the basis of the interference, the probability of detecting a target depends on the PDF of the target-plus-interference signal,  $p_{s+i}$ , which depends on the fluctuation statistics of both the interference and the target signals, as well as the SNR. The target detection probability  $P_D$  is the integral of the signal plus interference function from the threshold voltage to positive infinity.

$$P_D = \int_{V_t}^{\infty} p_{s+i}(v) dv \quad (3.6)$$

The total area under a PDF curve is always unity, so  $P_{FA}$  and  $P_D$  will be less than or equal to 1. If the target signal is larger than the noise signal by a great enough margin ( $\text{SNR} \gg 0$  dB), then the threshold can be set so that  $P_{FA}$  will be nearly zero, and yet  $P_D$  will be nearly unity. Required values of  $P_D$  and  $P_{FA}$  are determined from higher-level system requirements and can vary greatly. However, typically  $P_D$  is specified to be in the neighborhood of 50% to 90% for a  $P_{FA}$  on the order of  $10^{-4}$  to  $10^{-6}$ . Clearly if the interfering signal is of higher amplitude than the target signal ( $\text{SNR} < 0$  dB), then an unacceptably low  $P_D$  and high  $P_{FA}$  will result. In fact,  $P_D$  might be near zero and  $P_{FA}$  may be near unity. This condition would suggest using some signal processing technique to reduce or cancel the interference or enhance the target signal, increasing the SNR in either case.

### 3.3.1 Noise PDF and False Alarms

In the absence of any target signal, there is an opportunity for an interfering signal to be interpreted as a target signal. A false detection of such a noise signal, caused by the noise voltage exceeding the voltage threshold, is called a false alarm. To analytically determine the probability of false alarm for a given noise amplitude and threshold voltage, the probability density function (PDF) of the noise must be known. This requires an understanding of the noise statistics and detector design.

Most modern radar systems are coherent, and process the received signal as a vector with amplitude  $A$  and signal phase  $\phi$ . The most common detector circuit is a synchronous detector that develops the in-phase component of the vector (I), and the quadrature phase component (Q). Even in more modern systems in which the signal is sampled at the intermediate frequency (IF) with a single analog-to-digital (A/D) converter, the system firmware reconstructs the I and Q components of the signal for processing. When the interfering signal is thermal noise, each of these signals is a normally distributed random voltage with zero mean. The signal amplitude is found as

$$r = \sqrt{I^2 + Q^2} \quad (3.7)$$

Equation (3.7) is referred to as a *linear detector*, and the amplitude signal  $A$  is often called the radar *video* signal. It can be shown that when the I and Q signals are zero mean normal voltages as described above, the resulting noise amplitude is distributed according to the Rayleigh PDF [1]. In some systems the square root function is left out of Eq. (3.7), resulting in a *square-law* detector. In some legacy systems, mostly non-coherent ground mapping radars, the detected signal amplitude is processed by a logarithmic amplifier. In this case the detector is called a *log detector* and the output is sometimes called log-video. Log detectors were used to compress the wide dynamic range of the received signals to match the limited dynamic range of the display. Neither log nor square law detectors are as popular as the linear detector in modern radar systems. For this reason, the following analysis will be directed toward linear detection.

The Rayleigh PDF is

$$p_i(r) = \frac{r}{\sigma_n^2} \exp\left(\frac{-r^2}{2\sigma_n^2}\right) \quad (3.8)$$

where  $r$  is the detected envelope voltage and  $\sigma_n^2$  is the mean square voltage or variance of the noise, which is simply the noise power at the detector output. Figure 3-4 is a plot of the Rayleigh PDF, with an arbitrary, but reasonable location for a threshold voltage  $V_t$  plotted. By inspection, the particular threshold voltage shown would result in about 1%  $P_{FA}$ ; that is, it appears that about 1% of the area under the curve is to the right of the threshold. It should be understood that, for most systems, false alarms do occur. Seldom is a threshold established that is so far above the mean interference level that no interfering signal ever exceeds the threshold, because the resulting probability of detection for a given SNR is also reduced. Rather, an appropriate balance between  $P_D$  and  $P_{FA}$  is the goal. Normally, the probability of a false alarm is low. As an example, the system may be designed to produce, on average, one false alarm per complete antenna scan pattern.

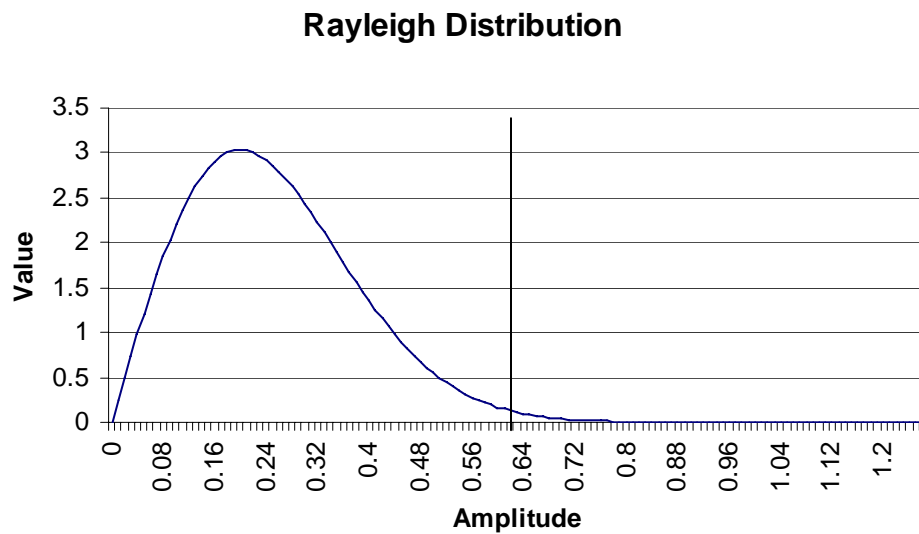


Figure 3-4. Rayleigh distribution with an arbitrary threshold



For a single sample of Rayleigh-distributed interference, the probability of false alarm is found from Eqs. (3.5) and (3.8):

$$P_{FA} = \int_{V_T}^{\infty} \frac{A}{\sigma_n^2} e^{-A^2/2\sigma_n^2} dA = e^{-V_T^2/2\sigma_n^2} \quad (3.9)$$

Solving for  $V_T$  provides the threshold voltage required to obtain a desired  $P_{FA}$ :

$$V_T = \sqrt{2\sigma_n^2 \ln(1/P_{FA})} \quad (3.10)$$

Thus, given knowledge of the desired  $P_{FA}$ , noise statistics, and detector design, it is possible to determine the threshold level that should be used at the detector output. Note that the target echo statistics are not involved in setting the threshold level.

Often search systems are designed such that if a detection is made at a given position for a given dwell, understanding that such detection may be a false alarm, a subsequent *confirmation* or *verification dwell* at the same position is processed, to see if the signal still exceeds the threshold. For a false alarm, the likelihood of a subsequent false detection is remote, settling the question of whether the detection was a false alarm or a true target. Even this process is not perfect, since there is still a remote likelihood that the false alarm will persist, or that a true target will not. Assuming that the probability that a false alarm will occur for each of  $n$  independent trials,  $P_{FA}(n)$ , is related to the single trial probability of false alarm,  $P_{FA}(1)$ , by

$$P_{FA}(n) = [P_{FA}(1)]^n \quad (3.11)$$

The likelihood that a false alarm will occur for two consecutive trials is  $P_{FA}^2$ , or for three trials  $P_{FA}^3$ , etc. As an example, for a single-trial  $P_{FA}$  of  $10^{-4}$ , the two-trial  $P_{FA}$  is  $10^{-8}$ .

Consider how the use of verification dwells affects the false alarm rate and search time for a hypothetical search radar. Continuing the example given earlier, suppose the radar has 90 beam positions for a given search sector, 333 range bins for each beam position, and 32 Doppler bins for each range/azimuth position. There will then be about 960,000 opportunities for a false alarm in a complete search scan (959,040 to be precise). For a single-dwell false alarm probability of  $10^{-5}$ , there will be about ten false alarms during the scan on average. The user normally has to determine the acceptable false alarm rate for the system, one that does not overload the signal processor or fill the display with false detections, making it difficult to sort out the desired detections. The use of a verification dwell after each regular dwell could reduce the overall  $P_{FA}$  to  $(10^{-5})^2 = 10^{-10}$  so that there would be a false alarm after verification only one in 100,000 scans, on average.

Continuing with the search example given in section 3.2.2, if each verification dwell requires 2 ms, the same as the regular dwells, then 10 verification processes will add approximately 20 ms to each nominally 540 ms search time. This is likely an acceptable expense, the alternative being to use a higher threshold voltage, which would reduce the probability of detection. However, if too many confirmation dwells are initiated, the radar search time would suffer significantly. For instance, if the  $P_{FA}$  were  $10^{-4}$ , then there would be about 100 false alarms per scan on average. The confirmation dwells would then add about 200 msec to every 540 ms dwell, a 37% increase in search time. This increase would probably be considered an inefficient use of time.

### 3.3.3 Signal Plus Noise PDF – Target Detection

If, at some point during the search, the radar antenna is pointed in the direction of a target, then at the appropriate range there will be a signal that results from the target. Of course, the interfering signal is still present, so the signal in the target cell is a combination of target plus the interference. This signal is the one the radar is intended to detect. Since it is comprised of a combination of two signals, one a varying interference signal, and the other a target signal, then there will be a variation to the composite signal.

Therefore, it has a PDF which is dependent on the target echo fluctuation properties as well as the interfering signal properties. Target fluctuations are characterized in Ch. 7 and their effect on detection is described in Ch. 15. Only the simpler case of a non-fluctuating target echo is considered here to illustrate detection concepts.

For a non-fluctuating target, the PDF of the target-plus-noise signal has originally been shown by Rice [2], and later discussed in [3] and [4] to be of the Rician form. This PDF is defined in Eq. (3.12) and plotted in Fig. 3-2, along with the interference-only Rayleigh PDF for comparison.

$$p_{sig}(r) = \frac{r}{\sigma_n^2} \exp\left[-(r^2 + r_{sig}^2) / 2\sigma_n^2\right] I_0(r r_{sig} / \sigma_n^2) \quad (3.12)$$

where

where:  $r_{sig}$  is the detected signal voltage

and  $I_0(\cdot)$  is the modified Bessel function of the first kind and zero order.

The procedure for determining the probability of detection given the target-plus-noise PDF, is the same as for determining  $P_{FA}$  given the noise-only PDF. Using the threshold determined from the noise statistics in Eq. (3.10), integrate the PDF from the threshold voltage to positive infinity:

$$P_D = \int_{V_t}^{\infty} p_{sig}(r) dr = \int_{V_t}^{\infty} \frac{r}{\sigma_v^2} \exp\left[-(r^2 + r_{sig}^2) / 2\sigma_v^2\right] I_0(r r_{sig} / \sigma_n^2) dr \quad (3.13)$$

This integral has no easy closed-form solution. Rather, it is defined as a new special function called *Marcum's Q function*,  $Q_M$ , discussed further in [5] and [17].

Routines to compute Marcum's Q function are available in MATLAB™ and similar computational systems. In addition, various analytic approximations for the calculation of ROCs for the case of a non-fluctuating target in noise are discussed in section 3.3.7 of this chapter.

For the case shown in Figure 3-5(a),  $P_D$  will clearly be significantly greater than the  $P_{FA}$ ; by inspection about 95%. That is, it appears that about 95% of the area under the “target” curve is to the right of the threshold. This figure also again makes clear that as the threshold is raised or lowered, both  $P_D$  and  $P_{FA}$  will be decreased (higher threshold) or increased (lower threshold).

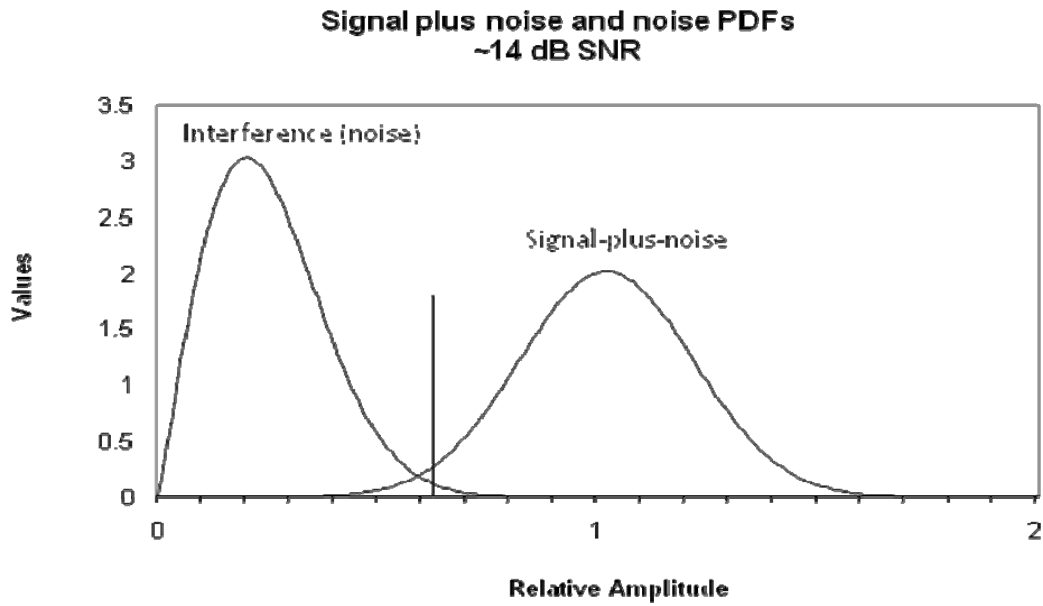


Figure 3.5(a). Noise-like distribution, with target-plus-noise distribution.

Moving the threshold to the left (lower) or right (higher) changes the  $P_D$  and  $P_{FA}$  together, for a given SNR. To get improved  $P_D$ , without increasing the  $P_{FA}$  requires that the two curves be separated more – a higher SNR is required. Figure 3-5(b) demonstrates that increasing the SNR, while maintaining the same threshold setting, increases the  $P_D$ . By observation, it appears that the  $P_D$  is higher than 99% for this case.

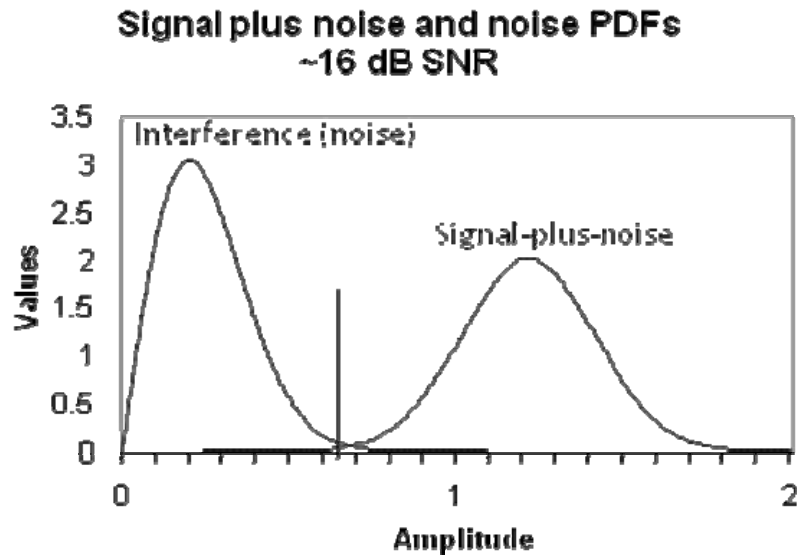


Figure 3.5(b). Noise-like distribution, with target-plus-noise distribution, demonstrating the higher  $P_D$  achieved with a higher SNR.

If the  $P_D$  and  $P_{FA}$  performance is not as good as required, that is, if the  $P_{FA}$  is too high for a required  $P_D$  or the  $P_D$  is too low for a required  $P_{FA}$ , then something must be done to better separate the interference and target PDFs on the plot. Either the noise has to be moved to the left (reduced in amplitude) or the target has to be moved to the right (increased in amplitude). Alternatively, the variance of the noise can be reduced, which will narrow both PDFs. These effects can only be made by modifying the system in some way to increase the SNR, either by modifying the hardware or applying additional signal processing. For example, the SNR can be increased by adjusting several of the terms in Eq. (2.20) in the preceding chapter. For example, the designer could increase the transmit power, the dwell time, or the antenna size (and thus gain).

Figure 3-5(a) shows the interference and target-plus-interference PDFs for a specific If the SNR were to increase, the two curves would exhibit more separation, and SNR.for a given threshold (constant  $P_{FA}$ ), it would be possible to increase the  $P_D$ . This effect is shown in Fig. 3-5(b). Conversely, if the SNR were to be reduced, then the curves would overlap more, and a lower  $P_D$  would result for a given threshold. This suggests that a curve of  $P_{FA}$  vs.  $P_D$  for given SNR, or of  $P_D$  vs. SNR for a given  $P_{FA}$  would be valuable.

### 3.3.4 Receiver Operating Curves

The plots shown above depict the PDFs for noise and target-plus-noise, with an arbitrary threshold voltage plotted. The calculations described above will produce the  $P_D$  and  $P_{FA}$  for a given threshold and SNR. If the threshold is varied, a series of combinations of  $P_D$  and  $P_{FA}$  result that describe the tradeoff between detection and false alarm probabilities for a given SNR. A succinct way to capture these tradeoffs for a large number of radar system operating conditions is to plot two of the three values  $P_D$ ,  $P_{FA}$ , and SNR with the third as a parameter. The receiver operating characteristic (ROC) is just such a curve. An example of a ROC is shown in Fig. 3-6, which presents a set of curves of *the SNR required to achieve a given  $P_d$* , with  $P_{FA}$  as a parameter, for a non-fluctuating target. Two alternative formats for the ROC curves are found in the literature. Some authors present: plots of  $P_D$  vs. SNR with  $P_{FA}$  as a parameter, while others present plots of  $P_D$  vs.  $P_{FA}$  with SNR as a parameter. A number of texts, for example [7-11], present ROC curves for a variety of conditions, most often for the case of non-fluctuating and Swerling fluctuating target signals in white noise. Results for other target fluctuation and interference models are available in the literature. These results are derived using the same general strategies described above, but differ in the details of the PDFs involved and thus the results obtained.

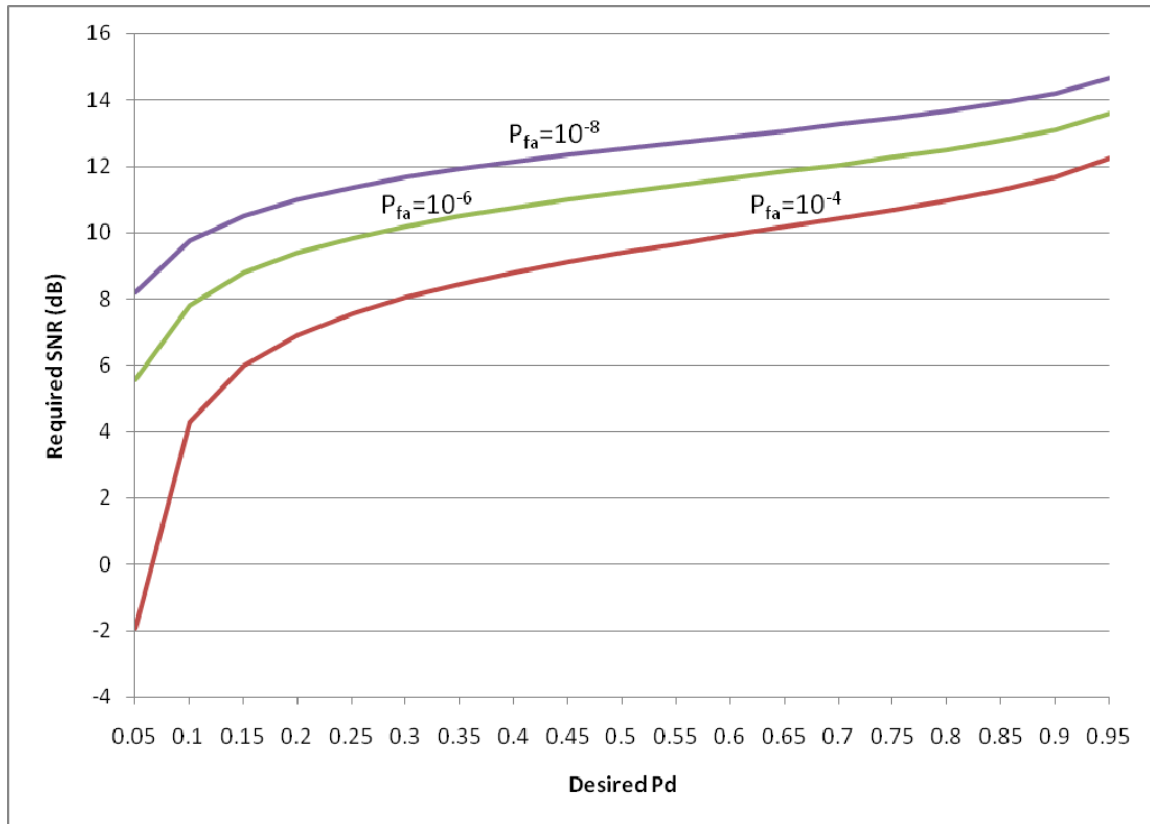


Figure 3-6. Receiver operating curves for non-fluctuating (SW0) target in noise (SNR vs.  $P_d$ ).

### 3.3.5 Fluctuating Targets

In addition to the fact that the noise interference signal fluctuates, it is also true that the target signal fluctuates for most real targets. Peter Swerling developed a set of four statistical models which describe four different target fluctuation conditions [8]. The four cases include two PDF models, (Rayleigh and Chi-square) and two fluctuation rates (dwell-to-dwell<sup>5</sup> and pulse-to-pulse.) They are labeled Swerling 1, 2, 3, and 4. Table 3.0 shows the PDFs and fluctuation characteristics for the four models. A non-fluctuating target is sometimes called a Swerling 0 or a Marcum target model. These, as well as other target models are discussed in detail in Chapter 7.

<sup>5</sup> Classically, the slowly fluctuating target was described as fluctuating from scan-to-scan, however, with modern system signal processing, the term dwell-to-dwell is often used.



Table 3-0. Swerling Models.

<b>Probability Density Function of RCS</b>	<b>Fluctuation Period</b>	
	<b><i>dwelt-to-dwelt</i></b>	<b><i>pulse-to-pulse</i></b>
Rayleigh	Case 1	Case 2
chi-square, degree 4	Case 3	Case 4

Table 3-1 gives some previously-calculated commonly-specified  $P_{FA}$  and  $P_D$  values, and the required SNR in dB for the five common target models. These points were extracted from plots in [11]. For a non-fluctuating target in noise-like interference, reliable detection (90%  $P_D$ ) is achieved with a reasonable ( $10^{-6}$ )  $P_{FA}$  given an SNR of about 13.2 dB. In the case of a fluctuating target signal, the PDF of the target plus interference is wider, leading to a lower  $P_D$  than for a non-fluctuating target at the same SNR. Thus, a higher SNR is required to achieve 90%  $P_D$ . In fact, an SNR of 17.1 to 21 dB is required for to achieve  $P_D = 90\%$  at  $P_{FA} = 10^{-6}$  vs. 13.2 dB for the nonfluctuating case. Lower SNR values provide lower detection probabilities, which may still be acceptable if detection can be made on the basis of several opportunities, such as over several antenna scans, or several consecutive dwelt periods. The system designer thus can trade radar sensitivity vs. observation time in the overall system design.

Table 3-1. Required SNR for various target fluctuation models.

	<u>Pd</u>	<u>SW0</u>	<u>SW1</u>	<u>SW2</u>	<u>SW3</u>	<u>SW4</u>
$P_{fa}=10^{-4}$	50	9.2	10.8	10.5	11	9.8
	90	11.6	19.2	19	16.5	15.2
$P_{fa}=10^{-6}$	50	11.1	12.8	12.5	11.8	11.8
	90	13.2	21	21	17.2	17.1

Chapter 14 describes the statistical nature of most target signals, showing that most targets of interest are usually fluctuating, rather than of fixed amplitude. Details of the calculation of  $P_D$  and  $P_{FA}$  and corresponding ROC curves for the fluctuating target cases are given there. Figure 3-7 is an example of the ROC curves for the Swerling 1 case. This can be compared to Fig. 3-6, which present the same data for the nonfluctuating target case.

Because the PDF of a fluctuating target is “spread” more than that of a non-fluctuating target, for a given SNR, the target and interference curves will overlap more. Therefore, for a given threshold setting, the  $P_d$  will be lower for the fluctuating target. Figure 3-8 shows the SNR as a function of  $P_D$  for a SW 0 (non-fluctuating) target and a SW 1 target. Notice that for levels of  $P_d$ , from 50% to 95%, the SNR required for a fluctuating target is significantly higher than that for a non-fluctuating target.

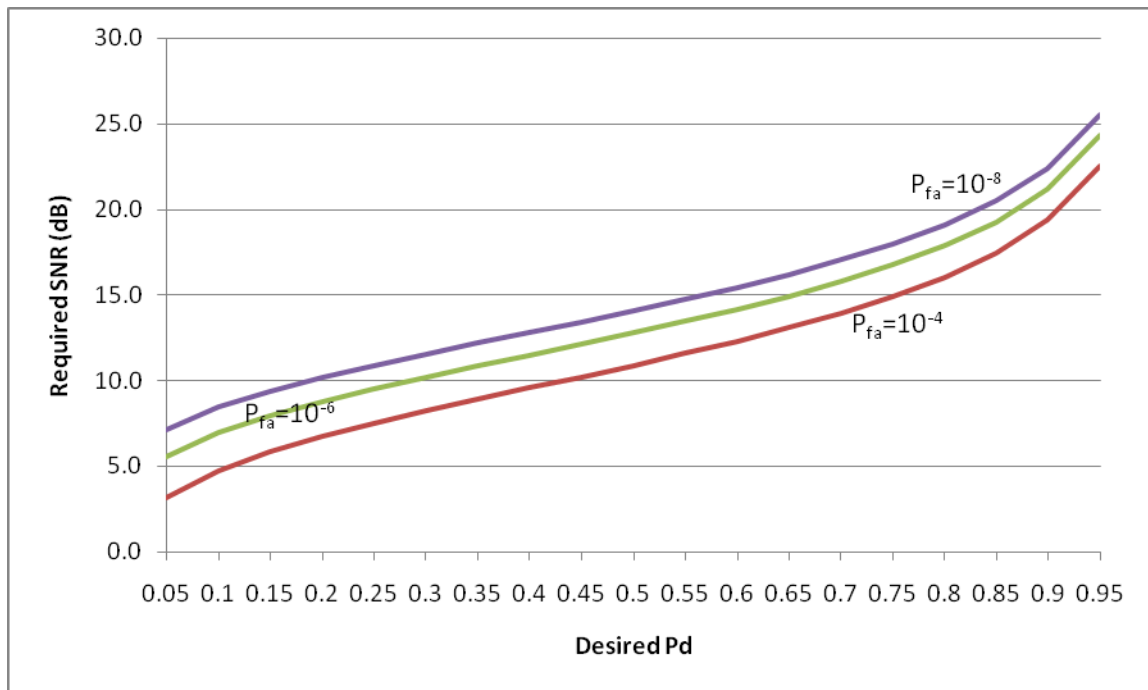


Figure 3-7. Receiver operating curves for fluctuating (SW1) target in noise (SNR vs.  $P_d$ ).

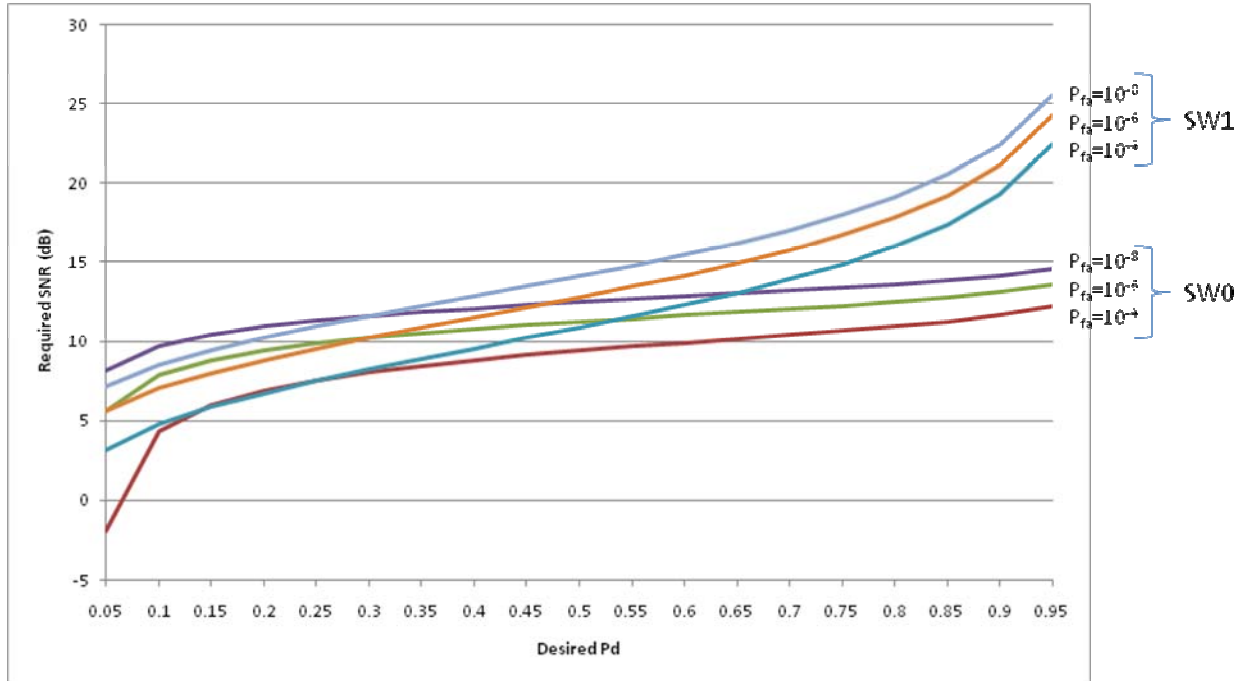


Figure 3.8. Required  $P_d$  vs. Desired SNR for non-fluctuating (SW0) and fluctuating (SW1) target models.

### 3.3.5 Interference Other Than Noise

The curves that have been plotted and presented in many standard radar texts give the  $P_D$  and  $P_{FA}$  for various SNR, where the interfering signal is Rayleigh-distributed after the linear detector. Thermal noise in the radar and noise jamming usually satisfy this condition. Clutter interference, on the other hand, usually does not. The PDFs for clutter are proposed in many radar texts and journal articles. Weibull, log-normal, K-distributed, and others are common models [12][13][14]. Chapter 6 provides a summary of the clutter statistics that one normally encounters in modern radars.

It is not the intent in this chapter to fully describe these models, however, it is the intent to build an appreciation for the effects of these fluctuation models on target detection statistics. In general, the nature of the PDFs for distributions associated with clutter is such that they have longer “tails” in the PDFs. That is, for a given mean value, there is a higher probability that the signal reaches higher amplitudes than that of noise, so that more of the area under the curve is to the right of the threshold. The effect is to increase the  $P_{FA}$  for a given threshold setting. If a given  $P_{FA}$  is to be maintained as the clutter signal begins to contribute to the total interference, the threshold must be increased to bring the  $P_{FA}$  back to the desired value. Doing so will also lower the  $P_D$  for a given signal-to-interference ratio because less of the area under the target curve will be to the right of the higher threshold. In Figure 3-9, a hypothetical but typical clutter PDF is plotted in addition to the Rayleigh distribution, to demonstrate the effect of the longer tail in the clutter distribution. The clutter distribution will produce a higher  $P_{FA}$  for the threshold setting shown. Therefore, the threshold will have to increase (move to the right) to recover the desired  $P_{FA}$ . This means that for a given target signal, the  $P_D$  will be lower than for the threshold setting associated with the Rayleigh distribution. In fact, depending on the particular clutter encountered, the effect of these extended tails can be severe. In some cases, to maintain a given  $P_{FA}$ , and  $P_D$ , the SIR must be 10 or even 20 dB higher than if the interference is noise-like. It is in these conditions that some method for reducing the clutter signal must be employed. Moving Target Indication (MTI) and pulse-Doppler processing techniques are the most common of these. These techniques, which are discussed in Ch. 17, reduce the clutter signal significantly

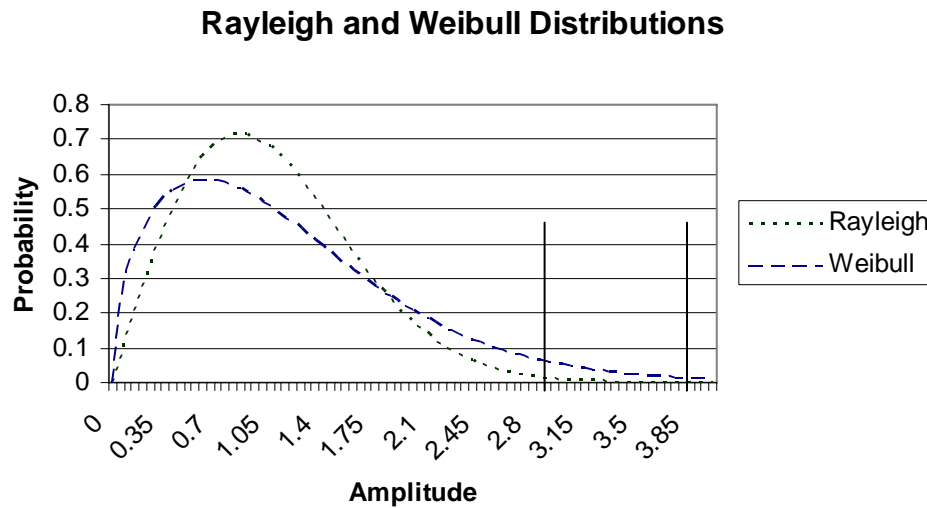


Figure 3-9. Example clutter PDF compared to noise.

The clutter signal is often significantly larger in amplitude than the target signal. This is because for a clutter cell illuminated by a given beamwidth and range resolution, the clutter area can be very large, which, when multiplied by the average reflectivity of the clutter in the cell, produces a large effective RCS. The target may be quite small, and for stealth targets, smaller yet. In this case, the target signal must be separated from the clutter signal in the spectral domain, usually employing pulse-Doppler (FFT) processing. Since it is impractical to completely confine the clutter signal to only a few Doppler bins, there will still be some residual clutter signal persisting in the vicinity of the target signal, and the question is: what is the shape of the residual clutter distribution curve after the processing? The central limit theorem would suggest that since 20 or 30 samples are integrated, the new distribution might be Gaussian. This requires that the individual interference samples are statistically independent. Are the samples independent? This depends on the PRF, the decorrelation time of the clutter, and the dwell time. For most cases, the samples are NOT independent, suggesting that the residual clutter signal after the processor is the same as the original distribution – e.g. Weibull.

### 3.3.6 Some Closed-Form Solutions

Exact calculation of the probability of detection requires solving the integral in Eq. (3.13) or, equivalently, evaluation of the Marcum  $Q$  function. While this is relatively easy using modern analysis tools such as MATLAB<sup>®</sup>, it is valuable to have a simple closed form solution for the mathematical procedures described above that can be solved using a spreadsheet or even a calculator. Fortunately, excellent approximations to the rigorous results using simple formulae are available. These approximations are applicable for estimates of SNR with precision on the order of 0.5 dB, and if extreme values of  $P_D$  and  $P_{FA}$  are not desired. In this chapter, Albersheim's approximation for nonfluctuating targets is presented. Also given is the exact results for a Swerling 1 target when only a single sample is used for detection. The cases summarized here provide examples of detection performance and demonstrate the advantage of multiple-dwell detection techniques.

#### *3.3.6.1 Approximate Detection Results for a Non-fluctuating Target*

Albersheim's equation [15] [16] is an empirically derived equation relating  $P_D$ ,  $P_{FA}$  the number of pulses noncoherently integrated ( $N$ ), and the single-pulse SNR. It applies to Swerling 0 (nonfluctuating) targets and a linear detector, though it also provides good estimates for a square law detector. This is a very good approximation for values of  $P_D$  between 0.1 and 0.9 and of  $P_{FA}$  between  $10^{-7}$  and  $10^{-3}$ . Figure 3-10 shows ROCs computed using Albersheim's equation for  $P_{FA}$  values of  $10^{-4}$  and  $10^{-6}$ . The figure also shows the exact results from [11]. Note the excellent agreement between the estimated and exact results for these cases.

Albersheim's estimate of the required SNR to achieve a given  $P_D$  and  $P_{FA}$  when  $N$  independent samples are noncoherently integrated is

$$SNR = -5 \log_{10} N + \left( 6.2 + \frac{4.54}{\sqrt{N + 0.44}} \right) \log_{10} (A = 0.12AB + 1.7B) \quad (3.14)$$

where:

$$A = \ln(0.62 / P_{FA}) \quad (3.15)$$

and

$$B = \ln \left( \frac{P_D}{1 - P_D} \right) \quad (3.16)$$

It is also possible to rearrange Albersheim's equation to solve for  $P_D$  given  $P_{FA}$ ,  $N$ , and the single-pulse SNR. Details are given in [19].

### SNR vs. Pdet for SW0

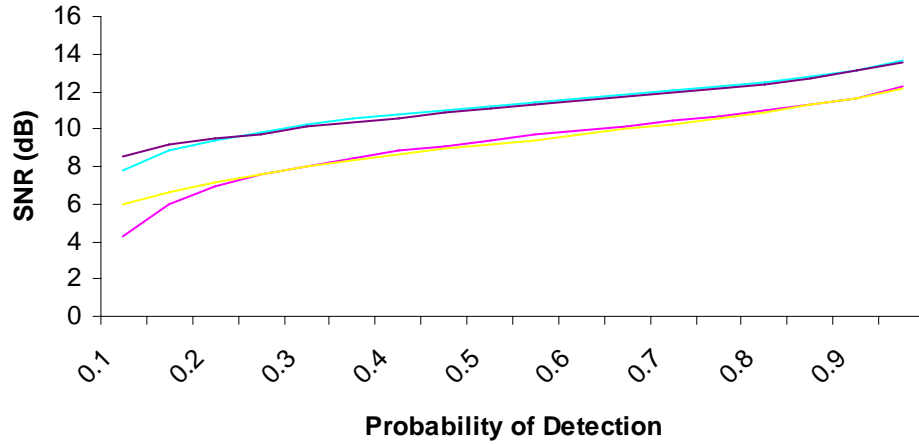


Figure 3-10. SNR vs.  $P_D$  for a Swerling 0 target using Albersheim's equation, plotted with tabulated results from Mayer and Meyer [11].

Though Albersheim's equation provides simple closed form method for calculation, it applies only to a non-fluctuating target, which is seldom a good model in practice. In Chapter 7, an approximation similar in spirit to Albersheim's equation, but applicable to all of the Swerling models, is presented.

#### 3.3.6.2 Swerling 1 Target Model

The Swerling models for describing the statistics of target fluctuations were described in Section 3.3.5. For the purpose of providing an example of a ROC for fluctuating targets, a Swerling 1 target model with a single echo sample (no noncoherent integration of multiple samples) will be considered here. Recall that a Swerling 1 target is described as having multiple scatterers of roughly the same RCS. The resulting PDF for this target is a Rayleigh distribution. In fact, this is the same distribution used to describe receiver noise. When combined with the Rayleigh noise distribution, the target+noise PDF is still a Rayleigh distribution. [22]. Specifically, the target+noise PDF is of the form:

$$p_{sig}(r) = \frac{r}{S + \sigma_n^2} \exp\left(\frac{-r^2}{2(S + \sigma_n^2)}\right), \quad (3.17)$$

where  $S$  is the mean target echo power and  $\sigma_n^2$  is the noise power. The probability of detection integral is

$$P_D = \int_{V_t}^{\infty} p_{sig}(r) dr = \int_{V_t}^{\infty} \frac{r}{S + \sigma_n^2} \exp\left[-\frac{r^2}{2(S + \sigma_n^2)}\right] dr \quad (3.18)$$

Computing this integral gives the probability of detection as

$$P_D = \exp\left[\frac{-V_t}{1 + SNR}\right] \quad (3.19)$$

where  $SNR = S/\sigma_n^2$ . Using (3.10) it can be shown that the relationship between  $P_D$  and  $P_{FA}$  for this case is the simple relationship

$$P_D = (P_{FA})^{\frac{1}{1+SNR}} \quad (3.20)$$

Equation (3.20) applies only to the case of a Swerling 1 target in white noise, with detection based on only a single sample.



### 3.3.7 Multiple Dwell Detection Principles – Cumulative $P_D$

To determine the dwell time required at each beam position, it is necessary to determine the signal-to-noise ratio required to achieve the desired  $P_D$  and  $P_{FA}$  for a target at maximum range. As an example, for a  $P_D$  of 90%, and  $P_{FA}$  of  $10^{-6}$  and a Swerling 2 target, the SNR required is 18 dB. Given the available average power, antenna gain, wavelength, minimum target RCS, receiver noise figure, system losses, and maximum range, Eq. (2.30) can be used to determine the dwell time to achieve the required SNR of 18 dB.

At first, it might seem that a  $P_D$  of 90% is not sufficient to detect a threat with adequate certainty. In fact, radar systems often combine the results from multiple opportunities to detect a target, improving the *cumulative detection probability* for  $n$  dwells,  $P_D(n)$  relative to the single-dwell probability  $P_D(1)$ . For example, if the probability of detection on a single dwell is  $P_D(1)$ , the probability of detecting the target at least once in  $n$  tries is

$$P_D(n) = 1 - (1 - P_D(1))^n \quad (3.21)$$

provided that the detection results on each individual dwell are statistically independent. If  $P_D(1) = 90\%$ , then the cumulative probability for 2 tries will be  $P_D(2) = 99\%$ , and for three tries will be  $P_D(3) = 99.9\%$ .

The use of multiple dwells to improve detection probability presents an opportunity for a tradeoff of radar sensitivity for time. For example, if a 99%  $P_D$  was required on a *single* dwell for the Swerling 2 example above, the SNR would have to be about 24 dB, about 6 dB higher than that required for 90%  $P_D$ . Using a second dwell with the 90%  $P_D$  doubles the time required to detect the target, but saves about 6 dB of radar sensitivity requirements. This translates into some combination of reduced transmit power, reduced antenna gain, or reduced signal processing gain requirements.

Of course, the false alarm probability is also affected by the use of multiple dwells. It is normally not desirable to have  $P_{FA}$  increase due to the multiple dwells, as  $P_D$  did. The equation for cumulative  $P_{FA}$  is the same as Eq. (3.21), with  $P_{FA}$  substituted for  $P_D$ . Because the single-dwell false alarm probability is usually a very small number, the results is well-approximated by the simpler equation

$$P_{FA}(n) \cong n \cdot P_{FA}(1) \quad (3.22)$$

Thus, for a 3-look cumulative  $P_{FA}(3)$  of  $10^{-6}$ ,  $P_{FA}(1)$  for a single dwell would have to be  $0.333 \times 10^{-6}$ . This modest reduction in the allowable single-dwell  $P_{FA}$  will increase the required SNR, but only be a small amount compared to the additional SNR that would be required to achieve a  $P_D$  of 99.9% in a single look.

### 3.3.8 $M$ out of $N$ Detection Criterion

Instead of detecting a target on the basis of at least one detection in  $n$  tries, system designers often require that some number  $m$  or more detections be required in  $n$  tries before a target detection is accepted. If  $m$  and  $n$  are properly chosen, this rule has the effect of both significantly reducing the  $P_{FA}$  and increasing the  $P_D$  compared to the single-dwell case. The probability of a threshold crossing on  $m$  or more out of  $n$  tries is found from the binomial distribution [20], [21]:

$$P(m, n) = \sum_{k=m}^n \frac{n!}{k!(n-k)!} P^k (1-P)^{n-k} \quad (3.23)$$

Here  $P$  is the probability of a threshold crossing on a single trial. Eq. (3.23) applies to both false alarm as well as detections. If  $P = P_{FA}(1)$ , then it gives the cumulative false alarm probability for an  $m$ -out-of- $n$  test; if  $P = P_D(1)$ , then it gives the cumulative detection probability for an  $m$ -out-of- $n$  test. For a commonly used set of 2 out of 3, (3.23) reduces to:

$$P(2,3) = 3P^2 - 2P^3 \quad (3.24)$$

and for 2 out of 4:

$$P(2,4) = 6P^2 - 8P^3 + 3P^4 \quad (3.25)$$

Figure 3-11 is a plot of the probability of detection or false alarm *vs.* single-dwell  $P_D$  or  $P_{FA}$ . Note that for typical single-dwell probabilities of detection (*i.e.* >50%) the cumulative  $P_D$  improves (increases), and for low probabilities of false alarm (*i.e.* <0.1) the  $P_{FA}$  also improves (is decreased). The only “cost” of this improvement is an extended dwell time for each beam position to collect the required data and conduct four detection tests instead of just one.

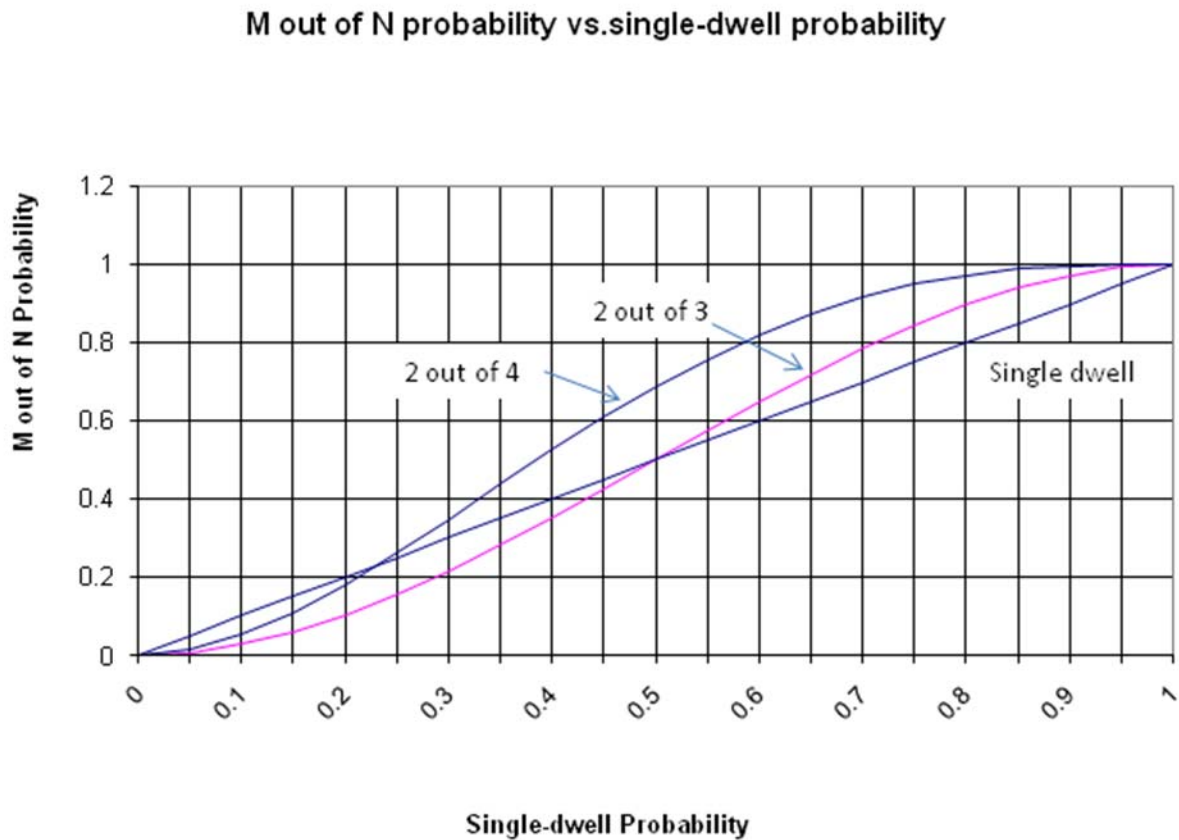


Figure 3-11. 2-out-of-3 and 2-out-of-4 probability of threshold crossing *vs.* single-dwell probability.

To get a better idea of the specific value of the effect of  $m$ -out-of- $n$  detection rules, Table 3-2 presents some specific examples of the effect on  $P_D$ , while Table 3-3 presents examples of the effect on  $P_{FA}$ . A single-dwell  $P_D$  of 0.9 and  $P_{FA}$  of  $10^{-3}$  provide fully adequate performance for most applications for 2 out of 4 scans.

Table 3-2.  $m$  out of  $n$  Probability of Detection compared to Single-Dwell Probability of Detection.

$P_D(1)$	$P_D(2,3)$	$P_D(2,4)$
1	1	1
0.95	0.993	.999
0.90	0.972	.996
0.85	0.939	.988
0.80	0.896	.973
.75	.844	.949
.70	.784	.916

Table 3-3.  $m$  out of  $n$  Probability of False Alarm compared to Single-Dwell Probability of False Alarm.

$P_{FA}(1)$	$P_{FA}(2,3)$	$P_{FA}(2,4)$
1	1	1
0.1	$2.8 \times 10^{-2}$	$5.23 \times 10^{-2}$
0.01	$2.98 \times 10^{-4}$	$5.92 \times 10^{-4}$
0.001	$2.998 \times 10^{-6}$	$5.992 \times 10^{-6}$
0.0001	$2.9998 \times 10^{-8}$	$5.9992 \times 10^{-8}$
0.00001	$3.000 \times 10^{-10}$	$5.9999 \times 10^{-10}$

It is sometimes the case that the multiple dwells are not collected on a single scan, but rather on successive scans. While this adds significant delay to the data collection

protocol and therefore the time to make a detection decision, for many applications this extra latency in the detection process is acceptable.

Some system applications require even larger numbers of dwells at a given beam position. For example, an airborne pulse-Doppler radar typically performs the search function in a high PRF mode so as to separate moving targets from wide clutter spectral characteristics. Consequently, the radar is highly ambiguous in range and there is a high likelihood of range eclipsing. Even in the medium PRF mode, there is likely to be range and Doppler aliasing and eclipsing. In order to improve the  $P_D$  and  $P_{FA}$  statistics in these conditions, often 6 or 8 dwells are used. Figure 3-12 shows the results of using Eq. (3.23) to compute the resulting  $P_D$  and  $P_{FA}$  for 3-out-of-6 and 3-out-of-8 detection rules. A single-dwell  $P_D$  of 90% results in a processed  $P_D$  of very close to 100% for these conditions. In this application, the  $m$ -out-of- $n$  rule is often combined with the use of *staggered PRFs*, discussed in Ch. 17.

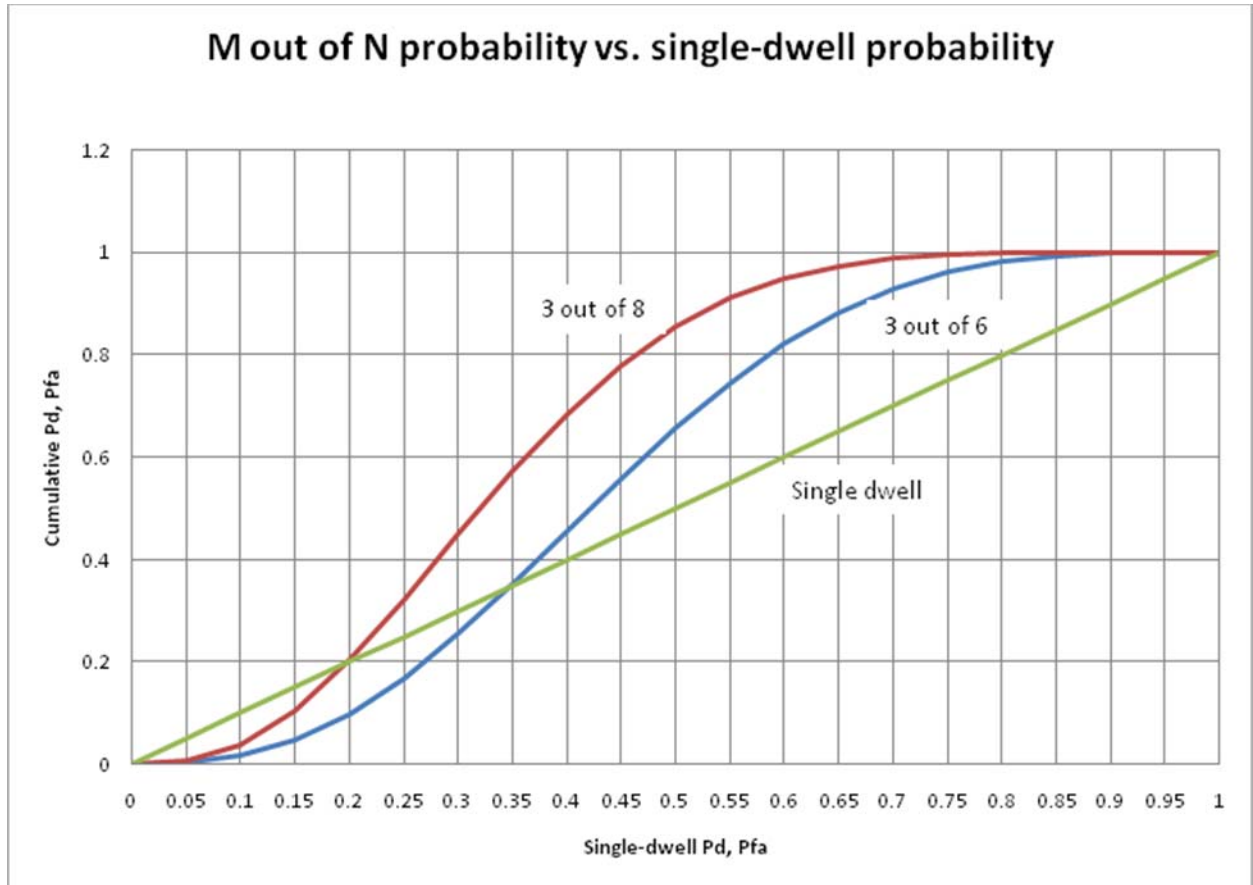


Figure 3-12. 3-out-of-6 and 3-out-of-8 probability of threshold crossing vs. single-dwell probability.

The question arises as to whether it is more efficient to use a relatively large number of dwells, which costs significant time, or to increase the single-dwell time. To examine this, consider the following example. Assume a  $P_D$  of 95% and a  $P_{FA}$  of  $10^{-6}$  is required for each complete scan. For a Swerling 1 target, the single dwell SNR must be 24 dB. Using Figure 3-12, it is seen that using 3 out of 6 processing, a cumulative  $P_D = 95\%$  and  $P_{FA}$  of  $10^{-6}$  can be achieved if the single-dwell  $P_D$  is about 70% and the single dwell  $P_{FA}$  is about 0.001. Using 3.20, it is seen that this performance can be obtained with a single-dwell SNR of only 12.5 dB.

This reduction of the required SNR by 11.5 dB (a factor of about 14) means that the radar can be “smaller” in some sense by a factor of 14. This could take the form of a reduction in average power, antenna gain, single dwell time, or relaxed restrictions on losses. For instance, although 6 dwells are now required, each one could be shorter by a factor of 14, reducing the overall time required to meet the detection specification. Taken a step further, 99%  $P_D$  can be achieved with 8 dwells and is equivalent to nearly 20 dB of additional radar sensitivity. Extending the time line by a factor of 8 can thus reduce the radar “size” by a factor of 100.

### **3.4 Further Reading**

More rigorous mathematical developments of the expressions for  $P_D$  and  $P_{FA}$ , as well as the general approach of threshold detection, are found in several radar texts, such as [6], [11], [17], and [23]. These references also extend the results discussed here to the effect of noncoherent integration of multiple samples prior to threshold testing.

Within this volume, target fluctuation models are discussed in more detail in Ch. 7. The application of the detection concepts discussed here to fluctuating target models is discussed in Ch. 15, which also provides the corresponding both exact expressions for  $P_D$  and  $P_{FA}$  for all of the Swerling models as well as an Albersheim-like approximation.

### **3.5 References:**

- [1] D. K. Barton, *Radar System Analysis*, Section 1.2. (Artech House, Dedham MA, 1976.)
- [2] S. O. Rice, Mathematical analysis of random noise, *Bell System Technical Journal* **23**, No. 3, July 1944, pp.282-332, and **24**, No. 1, January 1945, pp. 46-156.
- [3] J. V. DiFranco, and W. L. Rubin, *Radar Detection*, (Artech House, Dedham, MA., 1980, pp. 306-309.)

- [4] M. W. Long, *Airborne Early Warning System Concepts*, pp. 498-499, (Artech House, Dedham MA, 1992.)
- [5] A. Farina, *Radar Handbook*, Third edition, Chapter 24, Electronic Counter-countermeasures. (McGraw-Hill, New York, 2008.)
- [6] D. K. Barton, *Modern Radar System Analysis*, Section 2.2. (Artech House, Norwood, MA 1988.)
- [7] L. V. Blake, , *Radar Handbook*, Second Edition, Chapter 2. Prediction of Radar Range, pp. 2.20 – 2.24. (McGraw-Hill, New York, 1990.)
- [8] M. I. Skolnik, “Introduction to Radar Systems”, Third Edition, pg. 66, (McGraw Hill, New York, 2001.)
- [9] D. K. Barton, *Modern Radar System Analysis*, pp. 72-82. (Artech House, Norwood, MA. 1988.)
- [10] F. E. Nathanson, *Radar Design Principles*, 2<sup>nd</sup> ed., pp. 54, 83-86, 89-92. (McGraw-Hill, New York, 1991.)
- [11] D. P. Meyer, and H. A. Mayer, *Radar Target Detection, Handbook of Theory and Practice*. (Academic Press, New York, 1973.)
- [12] K. J. Sangston, and K. R. Gerlach, “Coherent Detection of Radar Targets in a Non-Gaussian Background”, *IEEE Transactions on Aerospace and Electronic Systems*, Vol. 30, No. 2, pp. 330-340, April 1994.
- [13] D. C. Schleher, “Radar Detection in Log-Normal Clutter”, *Proceedings IEEE International Radar Conference*, pp. 262-267, 1975.



- [14] F. Gini, M. V. Greco, and A. Farina, "Clairvoyant and Adaptive Signal Detection in Non-Gaussian Clutter: A Data-Dependent Threshold Interpretation", *IEEE Transactions on Signal Processing*, Vol. 47, No. 6, pp. 1522-1531, June 1999.
- [15] W. J. Albersheim, "Closed-Form Approximation to Robertson's Detection Characteristics," *Proceedings IEEE*, vol. 69, no. 7, p. 839, July 1981.
- [16] D. W. Tufts, and A. J. Cann, "On Albersheim's Detection Equation," *IEEE Trans. Aerospace and Electronic Systems*, vol. AES-19, no. 4, pp. 643-646, July 1983.
- [17] J. V. Difrancio and W. L. Rubin, *Radar Detection*, p. 313. (Artech House, Dedham, Ma., 1980.)
- [18] D. A. Shnidman, "Determination of Required SNR Values," *IEEE Trans. Aerospace & Electronic Systems*, vol. AES38(3), pp. 1059-1064, July 2002.
- [19] M. A. Richards, *Fundamentals of Radar Signal Processing*. (McGraw-Hill, New York, 2005.)
- [20] M. G. Bulmer, *Principles of Statistics*, p. 84. (Dover Publications, New York, New York, 1967.)
- [21] D. K. Barton, *Radar System Analysis*, p. 35. (ArtechHouse, Dedham, MA. 1976.)
- [22] D. K. Barton, C. E. Cook, P. Hamilton, *Radar Evaluation Handbook*, pg. 4-17, (Artech House, Dedham, MA. 1991.)
- [23] G. Minkler and J. Minkler, *CFAR, The Principles of Automatic Radar Detection in Clutter*, (Magellan Book Co., Baltimore, MD., 1990.)

## Problems

1a) For a mechanically scanned antenna having an azimuth beamwidth of 2 degrees and an elevation beamwidth of 3 degrees, how many beam positions are required to search a volume defined by a 90 degree azimuth sector and a 6 degree elevation sector?

Ans.  $45 \times 2 = 90$

1b) If the antenna were raster scanning at 180 degrees per second (that is, it is scanning in azimuth at 180 degrees per second), what is the maximum dwell time for each beam position? Assume it takes no time to change to a new elevation position, and it takes no time to change azimuth scanning direction.

Ans. 11.1 msec.

1c) For the conditions above, what is the total frame search time?

Ans. 1.0 seconds

2) For a phased array antenna, suppose the beamwidth at array normal is 2 degrees by 3 degrees (same as above). Also suppose that the dwell time used for scan angles between 0 and 30 degree is 4 msec, while for scan angles between 30 and 45 degrees it is 6 msec. If the beam position is stepped in equal step sizes, what is the total search frame time? Assume it takes negligible time to move from one position to the next.

$30 \times 4 + 16 \times 6 = 216$  msec.

3) What is the  $P_{FA}$  if the threshold voltage is set at 3 times the rms noise voltage?

4a) What threshold voltage is required to effect a  $P_{FA}$  of  $10^{-4}$  if the rms noise voltage is 150 mv?

4b) Assuming  $P_{FA} = 10^{-4}$ , how many consecutive verifications are required to effect a  $P_{FA}$  of  $10^{-9}$  or less?

Ans. Using (3.11):  $P_{FA}(n) = [P_{FA}(1)]^n$

More than two, but less than three, but using whole numbers, 3.

5) For a search volume that requires: 45 beam positions, 333 range bins, 32 Doppler bins, and a  $P_{FA}$  of  $5 \times 10^{-3}$ , how many false alarms occur on average in a single search frame?

Ans.  $45 \times 333 \times 32 = 479,520$

$479,520 \times 5 \times 10^{-3} = 2398$

6a) Consider a weapon locating radar having a beamwidth of 2 degrees in both azimuth and elevation (??) that is set up to search a volume defined by a 75 degree sector in azimuth and a 4 degree sector in elevation. If the radar also has a dwell time of 2.4 msec, and a plan to spend 5 dwells at each beam location, what is the total scan time?

Ans. 912 msec.

6b) If there are 8 targets being tracked, each consuming 6 milliseconds per track update at an update rate of 10 Hz (10 updates per second), what is the new search scan time?

Ans. 1.754 seconds

7a) Your enemy, 20 km distant, fires a mortar round in your general direction. The round has a vertical component of velocity of 200 meters per second. (Assume that this does not change during the engagement.) You are searching the area using a weapon locating radar. What must your maximum scan time be to insure at least four opportunities to detect the target before it passes through your 'search fence, which is the elevation sector extending from 0 to 4 degrees above the horizon?

Ans. 2 seconds

7b) If the round is detected at 2 degrees above the horizon, what must be the track sample rate be to get 50 track samples from between the point of detection and an elevation of 6 degrees above the horizon?

Ans. 6.25 Hz.

8) Given a radar system that has a single-dwell  $P_D$  of 50% and a single-dwell  $P_{FA}$  of  $5 \times 10^{-3}$ , what are the cumulative  $P_D$  and  $P_{FA}$  for 2 out of 3, and 2 out of 4 multiple dwell processes?

Ans. 2 out of 3: Using (2.24):  $P(2outof\ 3) = 3P^2 - 2P^3$

$$P_d(2/3) = 50\%$$

$$P_{fa}(2/3) = 7.5 \times 10^{-5}$$

and for 2 out of 4, using (2.25):  $P(2outof\ 4) = 6P^2 - 8P^3 + 3P^4$

$$P_d(2/4) = 68.75\%$$

$$P_{fa}(2/4) = 1.5 \times 10^{-4}$$

9) For a radar system that has a single-dwell  $P_D$  of 75% and a single-dwell  $P_{FA}$  of  $5 \times 10^{-3}$ , what are the  $P_D$  and  $P_{FA}$  for 2 out of 3, and 2 out of 4 multiple dwell processes?

Ans. 2 out of 3: Using (2.24):  $P(2outof\ 3) = 3P^2 - 2P^3$

$$P_d(2/3) = 84.4\%$$

$$P_{fa}(2/3) = 7.5 \times 10^{-5}$$

and for 2 out of 4, using (2.25):  $P(2outof\ 4) = 6P^2 - 8P^3 + 3P^4$

$$P_d(2/4) = 95\%$$

$$P_{fa}(2/4) = 1.5 \times 10^{-4}$$

10) Assuming that the target exhibits Swerling 1 fluctuations and that the  $P_{FA}$  that results from the multi-dwell (2 out of 4) processing in problem 10 is adequate, what SNR improvement is required to provide the same  $P_D$  and  $P_{FA}$  in a single dwell?

Ans. Using (3.20):  $P_d = \left(P_{fa}\right)^{\frac{1}{1+SNR}}$

The original SNR was 12.4 dB

The multiple-dwell SNR is equivalent to 22.3 dB.

9.9 dB increase in SNR would require that the dwell time, average power, or antenna gain be increased to provide 10 times the SNR.

11) Suppose a phased array search radar has to complete searching a volume defined by 10 degrees in azimuth, 10 degrees in elevation, and 40 km in range in 0.62 seconds. The range resolution is 150 meters, obtained with a simple 1 microsecond pulse width. At the center of the search sector, the antenna has a 2.7 degree azimuth beamwidth and a 2.7 degree elevation beamwidth. Since the target for which the system is searching is a moving target and there is surface clutter interfering with the detection, Doppler processing is used. There are 64 Doppler bins developed by the FFT processor. During a single search pattern, it is required that the probability of detecting a target is 99 percent, and on average one false alarm is allowed. What is the resulting  $P_D$  and  $P_{FA}$ , if the single-dwell  $P_D$  is 90% and the single-dwell  $P_{FA}$  is 0.01? If 3 out of 5 processing is employed, do the resulting  $P_D$  and  $P_{FA}$  meet the requirements?

Ans. Using (3.23):  $P(m \text{ out of } n) = \sum_{k=M}^N \frac{N!}{k!(N-k)!} P^k (1-P)^{N-k}$

For  $M=3$  and  $N=5$ , the resulting  $P_d$  is 99% and  $P_{fa}$  is  $9.9 \times 10^{-6}$